Mon. Not. R. Astron. Soc. **000**, 1–14 (2011) Printed 24 October 2011 (MN LATEX style file v2.2)

Accretion Discs Trapped Near Corotation

Caroline R. D'Angelo and Hendrik C. Spruit
Max Planck Institute for Astrophysics, Garching, Germany

24 October 2011

ABSTRACT

We show that discs accreting onto the magnetosphere of a rotating star can end up in a trapped state, in which the inner edge of the disc stays near the corotation radius, even at low and varying accretion rates. The accretion in these trapped states can be steady or cyclic; we explore these states over wide range of parameter space. We find two distinct regions of instability, one related to the buildup and release of mass in the disk outside corotation, the other to mass storage within the transition region near corotation. With a set of calculations over long time scales we show how trapped states evolve from both nonaccreting and fully accreting initial conditions, and also calculate the effects of cyclic accretion on the spin evolution of the star. Observations of cycles such as found here would provide important clues on the physics of magnetospheric accretion. Recent observations of cyclic and other unusual variability in T Tauri stars (EXors) and X-ray binaries are discussed in this context.

Key words: accretion, accretion discs – instabilities – MHD – stars: oscillations – stars: magnetic fields – stars:formation – stars:rotation

1 INTRODUCTION

Many accreting stars show evidence of the effects of a strong stellar magnetic field regulating the accretion flow onto the star. Accreting X-ray pulsars, for example, show flux modulation on timescales between $\sim 10^{-3} - 10^{3}$ seconds, which is attributed to the magnetic pole sweeping through our line of sight, illuminated by matter accreting along field lines (Davidson & Ostriker 1973). In some pulsars, this probe of the star's period has shown an evolution in the spin period of the star in time (e.g. Bildsten et al. 1997), which is attributed to the interaction with the surrounding material. On the other end of the energy scale, T Tauri stars also often have strong magnetic fields (up to 1-2 kG), and show some evidence that their period is regulated by the disc-field interaction (Getman et al. 2008).

From the earliest studies of stellar accretion researchers recognized that a strong magnetic field could substantially influence an accretion disc surrounding the star. Pringle & Rees (1972) estimated the 'magnetospheric radius' of the disc – the radius at which the magnetic field would truncate the disc – by equating the ram pressure of free-falling gas to the magnetic pressure of the field. The inner radius of the disc is thus determined by the magnetic field strength (assumed dipolar with a magnetic moment $\mu \equiv B_{\rm S} r_*^3$), stellar mass and the accretion rate onto the star: $r_{\rm m}^{7/2} \propto \mu^2 M_*^{-1/2} \dot{m}^{-1}$. The infalling material will then add its angular momentum to the star, causing it to spin faster. Illarionov & Sunyaev (1975) noted that if the magnetospheric radius extends beyond the corotation radius ($r_{\rm c} \equiv (GM_*)^{1/3}\Omega_*^{-3/2}$; where the Keplerian frequency of the disc equals the star's rotation frequency), the stellar magnetic field will spin faster than the gas at the inner edge of the disc, generally called the 'propeller' regime. A standard view expressed in the literature is that in this case the mass in the disc is expelled from the system (see below) and the star is spun down. The exact relationship between the spin evolution of the star and the accretion rate will depend on the physics of the disc-magnetosphere interaction when the inner edge of the disc is close to $r_{\rm c}$.

Although observations of magnetic accreting stars generally support this general picture for magnetospheric accretion, questions remain. A number of persistent X-ray pulsars show spin-down as well as spin-up (e.g. Bildsten et al. 1997), or a rate of spin-up much lower than expected based on the accretion rate. In addition, many sources show hysteresis, where the luminosity differs between spin-up and spin-down phases (Camero-Arranz et al. 2010), or even anti-correlates with spin-down (Chakrabarty et al. 1997). Finally, in persistent sources that show both spin-up and spin-down, the magnitude of $|\dot{\nu}|$ often stays nearly constant when the torque changes sign, which is not naturally explained in a model where the torque scales as a power of $\dot{m}$.

More recently, two transient X-ray pulsars were observed to undergo brief weak outbursts (lasting about 6-7 days) followed by a short period of quiescence (Heinke et al. 2010; Hartman, Galloway & Chakrabarty 2010). The outburst recurrence time (on the order of a month in both sources) is too short to be naturally explained by the ionization instability model (e.g. Lasota 2001), and Hartman, Galloway & Chakrabarty (2010) have suggested (based on the total outburst luminosity) that a significant amount of mass could remain stored in the disc when the accretion rate onto the star drops by at least 3-4 orders of magnitude. This explanation is inconsistent with the standard relation between accretion rate and inner radius, in which $r_{\rm in} \propto \dot{m}^{-2/7}$, so that a change of 10^4 in accretion rate corresponds to an increase of $\sim 10\times$ in $r_{\rm in}$.

In one of these sources, NGC 6440 X-2, Patruno et al. (2010)

recently reported the detection of a strong QPO at 1Hz. A similar QPO was previously detected in SAX J1808.4-3658 (Patruno et al. 2009). This QPO period is of the order $10^{-2} - 10^{-1}$ times the viscous timescale at the corotation radius $r_{\rm c}$ and hints further at interaction between the disc and the field.

Similar outburst time scales, in units of the viscous time scale, are seen in a class of young stars called 'EXors'. These stars typically show episodic changes in luminosity (of between 2-5 magnitudes) on timescales of a few years. The variability timescale implies accretion rate variability in the inner regions of the accretion disc, where it interacts with the magnetic field.

Together, these puzzling observations suggest that significant physics is missing in current interpretations of the phenomena seen in accreting magnetospheric systems.

1.1 Accretion at a centrifugal barrier

One of the things missing in the standard interpretation is the insight that mass prevented from accreting by the presence of a 'centrifugal barrier' does not necessarily have to leave the system at all. In other words, mass transferred from a binary companion onto a spinning magnetosphere does not have to be 'propellered' out.

This was already noted by Sunyaev & Shakura (1977) and Spruit & Taam (1993). Without mass loss, accretion on the magnetosphere can instead be *cyclic*, with periods of accumulation outside the corotation radius alternating with accreting phases. The problem of disc responding to the torque exerted at its inner edge by a spinning magnetosphere has a well-defined solution within the standard thin viscous disc formalism without mass loss. Mass loss in a magnetically driven wind may happen as well, but this bit of (still poorly known) physics is separate from the effect of a centrifugal barrier on a viscous disc.

We have studied this problem in D'Angelo & Spruit (2010) and D'Angelo & Spruit (2011) (hereafter DS10 and DS11 respectively). There we classified the properties of time dependent solutions of the thin disc diffusion equation with a magnetic torque acting at its inner edge (DS10), and studied the long term evolution of discs with such torques, including the spindown of the star (DS10).

Since the magnetic torques transport angular momentum outward, the density profile of the disc is altered substantially. The disc remains truncated only slightly outside $r_{\rm c}$ even when the accretion rate declines by several orders of magnitude. We found that the formation of a dead disc often results in the instability described by Spruit & Taam (1993), which we suggested could be operating in EXors as well as SAX J1808.4-3658 and NGC 6440 X-2. In the instability, the disc is initially truncated outside $r_{\rm c}$ and accretion is suppressed, causing material to build up in the inner regions of the disc. Eventually, the surface density in the disc becomes high enough to overcome the centrifugal barrier and accrete onto the star. Once the reservoir is emptied, the disc again moves outside $r_{\rm c}$ and the cycle begins again.

In DS10 we concluded that the presence of the instability depended on the mean accretion rate, $\dot{m}$ and the details of the disc-field interaction.We found that the uncertainties in the physics of the disc-field interaction could be parameterized into two independent, unknown (but constrained) length scales: the radial width of the region of interaction, Δr, and the length scale over which the disc moves from an accreting to a non-accreting state Δr_2. We made a preliminary investigation of the unstable solutions for different values of our independent parameters and found the shape and duration of the cycles of accretion varied widely. In the present work we investigate the parameter space more thoroughly in order to characterize the instability better and link it with observations.

1.2 Trapped discs

The modes of accretion of a viscous disc on a rotating magnetosphere can be classified in three states, all of which have a different appearance and effect on the star's evolution. We explicitly neglect the possibility of outflows, so that the disc never crosses into the propeller regime for any $\dot{m}$.

The disc state depends on the ratio of the mean accretion rate through the disc ($\dot{m}$) to the accretion rate that puts $r_{\rm in}$ at $r_{\rm c}(\dot{m}_{\rm c})$:

(i) $\dot{m} \gg \dot{m}_{\rm c}$: $r_{\rm in}<r_{\rm c}$, star spins up
(ii) $\dot{m} \simeq \dot{m}_{\rm c}$: $r_{\rm in}\approx r_{\rm c}$, star spins either up or down, inner edge stays near corotation while $\dot{m}$ varies.
(iii) $\dot{m} \sim 0$: $r_{\rm in}>r_{\rm c}$, star spins down, negligible accretion (dead disc).

State (ii) can be further divided into cases where accretion takes place in a continuous way, and cases where accretion is cyclic, with bursts of accretion alternating with quiescent phases. Our main interest in the following paper is this second case of cyclic accretion. If there is a long-term accretion rate imposed at the outer edge of the disc, as in a mass-transferring binary, dead disc states can occur as part of the cycle, as suggested by Sunyaev & Shakura (1977).

In DS11, we turned our attention to the long-term evolution of a viscous disc, and its effect on the spin evolution of the star. This added a new parameter to the problem, the moment of inertia I_* of the star, and introduced a new characteristic timescale, $T_{\rm SD}$, the spin-down timescale of the star.

When initial conditions are chosen such that $r_{\rm in}$ is initially inside $r_{\rm c}$, but moves gradually outward, we found that the evolution of the disc often gets 'trapped' with $r_{\rm in}$ near corotation, with a slowly decreasing accretion rate. The same happens when $r_{\rm in}$ is initially outside $r_{\rm c}$, but spindown of the star causes $r_{\rm c}$ to move out. When it catches up, $r_{\rm in}$ continues to hover slightly outside corotation as the two move outward. The outward angular momentum transport due to the magnetic torque is accompanied by low-level accretion onto the star. We called this phenomenon a 'trapped disc'. It is the intermediate state ii) mentioned above.

The disc does not stay trapped in all cases, however: $r_{\rm in}$ can also evolve well beyond $r_{\rm c}$ to become a 'dead disc' – the state iii) above. Whether or not the disc becomes trapped depends n the details of the disc-field interaction and on the ratio $T_{\rm visc}/T_{\rm SD}$ (where $T_{\rm visc}$ is the viscous accretion timescale of the disc at $r_{\rm c}$).

1.3 Observations and Spin Evolution of Stars with Trapped Discs

Accretion in the trapped state can be continuous or cyclic. In DS11 we limited ourselves mostly to parameter regimes that lead to continuous accretion, since the short time scale of the cycles makes it difficult to follow the long-term evolution of the disc. In this paper we study the cyclic case of trapped discs in more detail, with less emphasis on the system's long-term evolution. We study in particular the modification to the expected relationship between spin-down torque and luminosity, and the appearance of cyclic accretion.

We explore the nature and interpretation of these cycles in more detail here and study how the characteristics of the instability (such as its period and amplitude) change with the model parameters. These are discussed in section 4. When accretion is cyclic,

the torque between disc and magnetosphere varies over a cycle; its average over a cycle is what determines the net spindown or spinup torque on the star. In sec. 4.4 we study how this net torque differs from the steadily accreting case. Before that, in section 3 we discuss the observability of the quiescent "trapped disc", and the spin evolution of the star as a function of accretion rate.

In Sec. 5 we discuss our results in the context of the various observations mentioned above (persistent X-ray pulsars, the short recurrent outbursts in X-ray pulsars, and the episodic accretion bursts seen in both X-ray pulsars and young stars). We argue there that trapped discs may be related to a number of currently unexplained phenomena seen in magnetospherically accreting sources.

2 THE MODEL FOR MAGNETOSPHERIC ACCRETION

We briefly summarize the characteristics of our model for magnetospheric accretion, reviewing our description of the disc-field interaction and how this alters the structure of the disc when $r_{\rm in} > r_{\rm c}$. For a compact description see DS11; for more detail and our numerical implementation see DS10.

As mentioned above, the interaction between an accretion disc and magnetic field is likely confined to the innermost regions of the disc, so that most of the disc is shielded from the field. The coupling between the disc and the field distorts the field lines by differential rotation, which generates a toroidal field component and exerts a magnetic torque on the disc. In a very short time, the field lines become sufficiently distorted that they inflate and open, which can temporarily sever the connection between the field and disc, before reconnection events reestablish connection with the star. As a result, the variations in the magnetic field associated with the magnetosphere interaction will take place on timescales of order the rotation period of the star, P_* (Aly 1985; Hayashi, Shibata & Matsumoto 1996; Miller & Stone 1997; Goodson, Winglee & Boehm 1997); much shorter than the cycle times, which take place on a variety of viscous time scales in the disc.

It is sufficient to adopt a time-averaged value for the strength of the generated toroidal field component, $\eta \equiv B_\phi/B_z$ and the width of the interaction region $\Delta r/r_{\rm in}$. The size of the interaction region is unknown, so it is a free parameter in our model; we assume only that $\Delta r/r < 1$, and explore values in the range suggested by numerical simulations. (For a more extensive discussion of time variability in η and Δr see DS10.)

When the inner edge of the disc $r_{\rm in}$ is outside corotation $r_{\rm c}$, a magnetic torque T_B acts at the inner edge. The condition that this torque is transmitted outward by the viscous stress requires:

$$3\pi\nu\Sigma(r_{\rm in})r^2\Omega_{\rm K}(r_{\rm in}) = T_B. \quad (1)$$

This yields a boundary condition on the surface density at $r_{\rm in}$. When $r_{\rm in}$ is inside $r_{\rm c}$ however, the viscous torque and the surface density at $r_{\rm in}$ vanish: the standard case of a viscous disc accreting on a slowly rotating object applies. The viscous torque at $r_{\rm in}$ thus varies rapidly over the transition width Δr around $r_{\rm c}$. This can be taken into account in (1) by making T_B a function of $r_{\rm in}$,

$$T_B = y_\Sigma(r_{\rm in})T_0, \quad (2)$$

where y_Σ is a suitably steep function with the property that it varies from 0 to 1 over the width Δr: $y_\Sigma \to 0$ for $r_{\rm c} - r_{\rm in} \gg \Delta r$, $y_\Sigma \to 1$ for $r_{\rm in} - r_{\rm c} \gg \Delta r$. For T_0 we approximate the field strength at $r_{\rm in}$ as that of the star's dipole component, so the magnetic torque exerted by the field is

$$T_0 = \eta\,\mu^2\Delta r/r^4, \quad (3)$$

where μ is the star's dipole moment and η a coefficient of order unity. For numerical reasons, it is important that y_Σ be a smooth function; we use a $1 + \tanh$-profile of width Δr. For the viscosity we use a fixed radial dependence, $\nu = k_\nu r^{1/2}$, corresponding to an α-disc of constant α and aspect ratio H/r.

When $r_{\rm in} < r_{\rm c}$ the disc can accrete onto the star. The position of the inner edge of the disc is then related to the accretion rate. We use a standard estimate (Spruit & Taam 1993), which equates the magnetic torque with the torque needed to keep the accreting mass corotating with the star. It can be written as

$$\dot m_{\rm a} = \frac{\eta\mu^2}{4\Omega_* r_{\rm in}^5} \quad (4)$$

(the subscript $_{\rm a}$ stands for 'only in the case of accretion') and holds only for $r_{\rm in}<r_{\rm c}$. For $r_{\rm in}>r_{\rm c}$, the accretion rate drops to zero due to the centrifugal barrier. The relation between $r_{\rm in}$ and $\dot m$ thus also changes steeply around $r_{\rm c}$. This is another critical element that needs to be taken into account. We incorporate it by writing:

$$\dot m_{\rm co}(r_{\rm in}) = y_m(r_{\rm in})\dot m_{\rm a}(r_{\rm in}) \quad (5)$$

where $y_m(r_{\rm in})$ describes the steep variation in the transition zone, and $\dot m_{\rm co}$ is the mass flux *measured in frame comoving with the inner edge of the disc*:

$$\dot m_{\rm co} = \dot m + 2\pi r_{\rm in}\Sigma(r_{\rm in})\dot r_{\rm in}, \quad (6)$$

where $\dot r_{\rm in}$ is the rate of change of the inner edge radius (the distinction between $\dot m$ and $\dot m_{\rm co}$ was a crucial point missing in the formulation of ST93). For the 'connecting function' y_m, with limiting values 1 inside corotation and 0 outside, we again use a smooth $\tanh$- function. The width of this transition must be of the same order as the transition width Δr introduced above, but the physics determining it is rather different, so we keep it as a separate parameter Δr_2, and explore it independently.By introducing Δr and Δr_2 as the transition length scales from one boundary condition to other, we reduce the uncertainties of the transition region to two free but constrained parameters, which we vary systematically to explore the range of unstable solutions.

Eq. (4) and (6) define an equation for $r_{\rm in}(t)$. Together with the standard thin disc diffusion equation, we have a set of equations, second order in time and space, for Σ and $r_{\rm in}$. The equations are stiff inside corotation since one of the time derivatives (for $r_{\rm in}$) disappears. A numerical method appropriate for this circumstance has to be used.

The steady-state case, $\partial_t = 0$, is illustrative. The solution of the thin disc diffusion equation can be written as

$$3\pi\nu\Sigma = \frac{T_B}{\Omega(r_{\rm in})r_{\rm in}^2}\left(\frac{r_{\rm in}}{r}\right)^{1/2} + \dot m\left[1 - \left(\frac{r_{\rm in}}{r}\right)^{1/2}\right], \quad (7)$$

where T_B is given by (2) and $\dot m$ by (4, 6).

For $r_{\rm in}$ well outside corotation ($r_{\rm in}$ - $r_{\rm c} \gg \Delta r$), $\dot m$ vanishes and we have a dead disc. The surface density is then determined by the first term on the RHS. The steady outward flux of angular momentum in this case has to be taken up by a sink at some larger distance, otherwise the disc could not be stationary as assumed. This sink can be the orbital angular momentum of a companion star, or the disc can be approximated as infinite. The latter is a good approximation for changes in the inner regions of the disc, if we consider short time scales compared with the viscous evolution of the outer disc.

2.1 Characteristic numbers

We choose $r_{\rm c}$ (the star's initial co-rotation radius) for our length scale, and define $t_{\rm c} \equiv \nu/r_{\rm c}^2$, the viscous accretion timescale at $r_{\rm c}$ as our characteristic timescale. We adopt $\nu_0 \equiv \alpha\,(H/r)^2 = 10^{-3}$ for the dimensionless viscosity parameter, and $\eta = 0.1$ as the relative size of the B_ϕ component. We also define a characteristic accretion rate $\dot{m}_{\rm c}$:

$$\dot{m}_{\rm c} \equiv \frac{\eta\mu^2}{4\Omega_* r_{\rm c}^5}, \tag{8}$$

This is the accretion rate in (4) that would put the magnetospheric radius at $r_{\rm c}$.

For a typical ms-pulsar:

$$\dot{m}_{\rm c} = 10^{-14} M_\odot {\rm yr}^{-1} \left(\frac{M_*}{1.4M_\odot}\right)^{-5/3} \left(\frac{B_s}{10^8{\rm G}}\right)^2 \left(\frac{R_*}{10^6{\rm cm}}\right)^6 \left(\frac{P_*}{100\ {\rm ms}}\right)^{-7/3}, \tag{9}$$

while for the case of a T Tauri star disc,

$$\dot{m}_{\rm c} = 1.4\times 10^{-9} M_\odot {\rm yr}^{-1} \left(\frac{M_*}{0.5M_\odot}\right)^{-5/3} \left(\frac{B_s}{1500{\rm G}}\right)^2 \left(\frac{R_*}{2R_\odot}\right)^6 \left(\frac{P_*}{7\ {\rm d}}\right)^{-7/3}. \tag{10}$$

To characterize the spin change of the star, we adopt a characteristic torque based on the definition for $\dot{m}_{\rm c}$:

$$\dot{J}_{\rm c} \equiv \dot{m}_{\rm c}(GM_* r_{\rm c})^{1/2}, \tag{11}$$

which is the rate at which angular momentum is added by mass accreting at $\dot{m}_{\rm c}$. This definition is somewhat arbitrary, but has the advantage of being independent of $\Delta r/r_{\rm in}$ and $\Delta r_2/r_{\rm in}$.

3 SPIN EVOLUTION AND PHYSICAL PROPERTIES OF A TRAPPED DISC

3.1 Observability of trapped discs

The density structure of a trapped disc deviates from the standard accreting disc. In a dead disc (the limiting case of a trapped disc), the accretion rate is zero and the surface density profile is determined by the rate of angular momentum transport from the star to the disc.

Provided that the thin disc approximation remains a good description for the disc, meaning that the energy generated by viscous turbulence is dissipated locally the temperature of the dead disc can be estimated (Sunyaev & Shakura 1977) from the viscous dissipation.

The local energy dissipation rate in a viscous disc is:

$$Q^+ = \nu\Sigma(r\Omega_{\rm K}')^2 \;=\; \frac{9}{4}\nu\Sigma\Omega_{\rm K}^2. \tag{12}$$

Near the inner edge of the disc where most of the energy is dissipated, the disc can be approximated as steady, so (7) applies. For a dead disc ($\dot{m} = 0$ and $r_{\rm in}$ well outside corotation), $T_B = T_0$, and the surface density as a function of r is given by

$$\nu\Sigma = \frac{1}{3\pi}\left(\frac{T_0}{\Omega r^2}\right)_{r=r_{\rm i}} \left(\frac{r_{\rm i}}{r}\right)^{1/2}. \tag{13}$$

If this energy is radiated locally as a blackbody, then

$$Q^+ = Q^- = 2\sigma T_{\rm s}^4, \tag{14}$$

where $T_{\rm s}$ is the surface temperature of the disc as a function of radius (the factor 2 arising because the energy is lost from the two surfaces of the disc), and $\sigma_{\rm B}$ the Stefan-Boltzmann constant. With (3,13) this yields

$$\sigma_{\rm B} T_{\rm s}^4 = \frac{3}{8\pi}\eta\mu^2 \left(\frac{\Delta r}{\Omega r^6}\right)_{r=r_{\rm i}} \frac{GM}{r^3}\left(\frac{r_{\rm i}}{r}\right)^{1/2}, \tag{15}$$

which varies with r as $r^{-7/2}$, showing that most of the energy is radiated away near the inner edge by the mass piled up at the 'centrifugal barrier'. If $\nu \sim r^{1/2}$ as we assume in the calculations to follow, (15) implies $T_{\rm s} \sim r^{-1}$.

With the nominal object parameters used in 2.1, a dead disc with its inner edge near corotation will have a maximum temperature, at $r_{\rm in}$, of $T_{\rm s} \approx 300K$ in the case of a T Tauri star and $T_{\rm s} \approx 20000$ K for a ms X-ray pulsar. This estimate, however, only includes the internal energy dissipation in the disc. Both in protostars and X-ray binaries, reprocessing of radiation from the central object by the disc usually dominates over internal dissipation, especially at larger distances from the centre. Nonetheless, it might be possible to identify a disc as belonging to the dead class with more detailed information on the spectral energy distribution.

3.2 Accretion rate and angular momentum exchange with the star

The interaction between the magnetic field and the disc outside $r_{\rm c}$ removes angular momentum from the star, while the gas accreting onto the star spins it up. The net torque on the star is thus a function of both the average accretion rate through the disc and the location of $r_{\rm in}$. It is given by:

$$\dot{J} = \dot{m}(GM_* r_{\rm in})^{1/2} - \frac{\eta\mu^2}{r_{\rm in}^3}\frac{\Delta r}{r_{\rm in}} y_\Sigma, \tag{16}$$

where the first term gives the spin-up from accretion and the second term is the spin-down from the disc-field interaction. (The spin-down torque vanishes for $r_{\rm in} < r_{\rm c}$, which we impose with the y_Σ smoothing function.) In sec. 2 we defined the relationship between $\dot{m}$ and $r_{\rm in}$, so that $\dot{J}$ will just be a function of $\dot{m}$, $\Delta r/r_{\rm in}$ and $\Delta r_2/r_{\rm in}$. In the rest of the section we illustrate the implications of this relationship for the spin-evolution of the star.

Fig. 1 shows the relationship between $r_{\rm in}$ and $\dot{m}$ as $\Delta r_2/r_{\rm in}$ changes, to demonstrate how the disc can become trapped. The three curves show $r_{\rm in}$ as a function of $\dot{m}$ for $\Delta r_2/r_{\rm in} = 0.05$ (solid blue), 0.1 (dashed green) and 0.5 (triple-dot dashed red). At high accretion rates ($r_{\rm in} < r_{\rm c}$), all three curves scale as $r_{\rm in} \propto \dot{m}^{-1/5}$. However as $\dot{m}$ decreases the solutions quickly diverge. For small $\Delta r_2/r_{\rm in}$ ($\Delta r_2/r_{\rm in}$ =[0.05, 0.1]), there is a knee in the solution around $r_{\rm in} = r_{\rm c}$, and $r_{\rm in}$ increases much more slowly as $\dot{m}$ decreases, so that $r_{\rm in}$ remains close to $r_{\rm c}$ even when $\dot{m}$ has decreased by several orders of magnitude. For $\Delta r_2/r_{\rm in} = 0.5$, the knee straightens out since the transition from accreting to non-accreting solutions is much more gradual.

Fig. 2 shows the dependence of the net torque $\dot{J}$ on the star on accretion rate $\dot{m}$, for different values of $[\Delta r, \Delta r_2]$. At high accretion rates, the disc is strongly accreting, star spins up with the torque $\dot{J} \propto \dot{m}^{9/10}$. At lower accretion rates, the interaction region moves outside $r_{\rm c}$, causing the net angular momentum exchange to change sign, and spinning the star down. As the accretion rate decreases further and $r_{\rm in}$ moves increasingly far outside $r_{\rm c}$ into the effectively 'dead' state, the spindown torque decreases because of the decline of the star's field strength with distance.

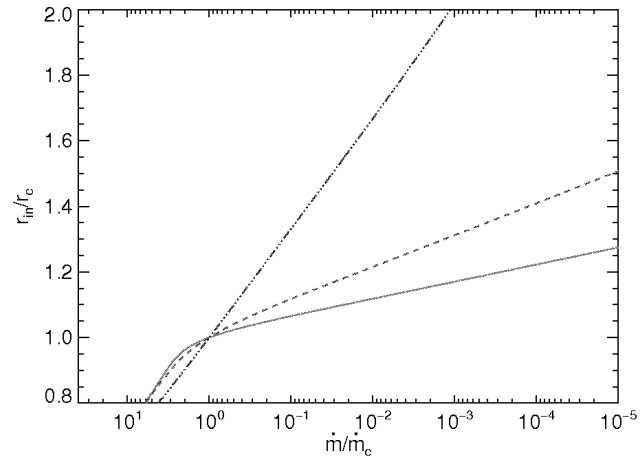

Figure 1. Change in $r_{\rm in}$ as a function of $\dot{m}$ for different $\Delta r_2/r_{\rm in}$. Solid curve: $\Delta r_2/r_{\rm in} = 0.05$, Dashed curve: $\Delta r_2/r_{\rm in} = 0.1$,Triple-dot-dashed curve: $\Delta r_2/r_{\rm in} = 0.5$

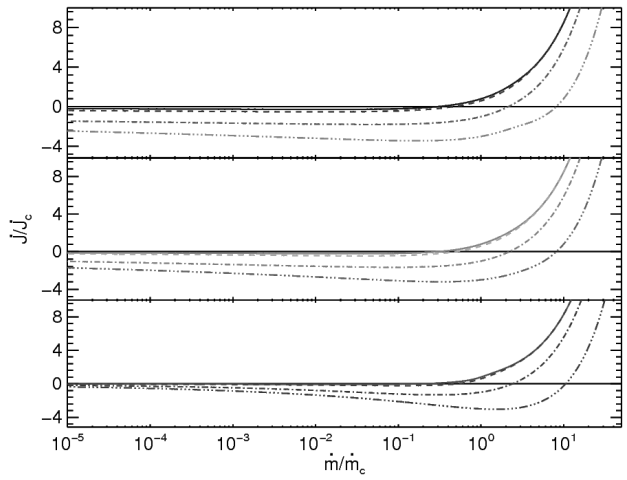

Figure 2. Change in net torque on the star as a function of $\dot{m}$ for different values of $\Delta r/r_{\rm in}$ and $\Delta r_2/r_{\rm in}$. From top to bottom, the individual panels correspond to $\Delta r_2/r_{\rm in} = [0.05, 0.1, 0.5]$. The different patterned lines correspond to different values of $\Delta r/r_{\rm in}$: 0.05 (solid), 0.1 (dashed), 0.5 (dot-dashed), and 1.0 (triple-dot dashed).

The detailed shape of the curves in figs. 1,2 reflects the ($\tanh$-) shape of the transition functions y_Σ and y_m we have used. More generally, however, when $\dot{J} < 0$, the amount of spin down is directly proportional to $\Delta r/r_{\rm in}$, and $\Delta r_2/r_{\rm in}$ determines how far away from $r_{\rm c}$ the disc can move as $\dot{m}$ decreases.

4 CYCLIC ACCRETION

The possibility of identifying cycles like those seen in DS10 in actual observations is a interesting prospect. Cycles would provide a direct observational connection with the trapped disc state phenomenon that we have identified here as a likely consequence of the disc-magnetosphere interaction. The shape of the cycles and circumstances of their occurrence would provide important clues about the details of the interaction region, which we have simply parametrized with the two transition widths $\Delta r/r_{\rm in}$(for the torque) and $\Delta r_2/r_{\rm in}$ (for the mass flux).

In this section we expand the analysis in DS10 to investigate the properties of the instability more quantitatively. In Sec. 4.1, we investigate the presence of the instability as a function of the system parameters. In sec. 4.2 we show how the period and amplitude vary with $\dot{m}$, $\Delta r/r_{\rm in}$ and $\Delta r_2/r_{\rm in}$. In sec. 4.4 we investigate how the presence of cycles will change the spin evolution of the star in comparison to a steadily accreting disc. Finally, in sec. 4.5 we examine the appearance of cycles for non-steady accretion in systems in which the star's spin is evolving.

4.1 Parameter map of the instability

In DS10 we showed that the disc instability depends on $\Delta r/r_{\rm in}$, $\Delta r_2/r_{\rm in}$ and $\dot{m}$, and ran simulations in the parameter spaces $[\Delta r, \dot{m}]$ and $[\Delta r_2, \dot{m}]$ to determine when the instability occurred. Additional simulations of trapped discs at very low accretion rates show the instability is present for a larger parameter space than we investigated in DS10, so here we have repeated our analysis on a larger parameter space and better-sampled grid.

As in DS10, we keep the rotation rate of the star fixed, since the time scale of the cycles is much shorter than the time scale of spin changes of the star. The corotation radius is then a fixed distance, and defines a unit of mass flux, $\dot{m}_{\rm c}$ given in sec. 2.1. As unit of length we can use $r_{\rm c}$, and as unit of time the viscous time scale $r_{\rm c}^2/\nu(r_{\rm c})$. Apart from a parameter specifying the radial dependence of ν, which we keep fixed throughout, the problem is then defined by the three dimensionless parameters $\Delta r/r_{\rm in}$, $\Delta r_2/r_{\rm in}$, and $\dot{m}/\dot{m}_{\rm c}$.

It turns out (discussed below) that this 3-dimensional parameter space contains 2 nearly separate regions of instability, which can be characterized using a few 2-dimensional slices instead of having to scan the entire space.

In comparison to DS10, the present results survey a larger parameter range at higher resolution for all three variables. The individual simulations at higher spatial and time resolution. In total we ran 1545 simulations: 855 in a 2-dimensional slice $[\Delta r, \dot{m}]$, and 690 in a $[\Delta r_2, \dot{m}]$ slice. Our goal was to determine the regions in parameter space where cyclic behaviour occurs, as well as how the characteristics of the cycles (such as period, amplitude and appearance) change as a function of the parameters.

Figures 3 and 4 show the unstable regions across $[\Delta r, \dot{m}]$ and $[\Delta r_2, \dot{m}]$. In fig. 3, we kept $\Delta r_2/r_{\rm in}$ fixed at 0.014 and surveyed the range $\Delta r/r_{\rm in} = [0.02, 0.28]$ and $\dot{m}/\dot{m}_{\rm c} = [10^{-6}, 6]$. Figure 4 surveys the same range in $\dot{m}$ and the range $\Delta r_2/r_{\rm in} = [0.004, 0.14]$, keeping $\Delta r/r_{\rm in}$ fixed at 0.05. The figures (especially figure 4) show that there are two distinct regions in which the instability is active, which we call RI and RII.

The instability has different properties in the two regions: the period, shape and amplitude of the outburst are all qualitatively different, as we demonstrate further below.

The first instability region (RI) appears in a small range of $\Delta r_2/r_{\rm in} = [0.002, 0.03]$, but over a considerable range in $\Delta r/r_{\rm in}$ (up to 0.25) and five orders of magnitude in accretion rate: $\dot{m}/\dot{m}_{\rm c} \simeq [10^{-6}, 10^{-1}]$. This instability region was the focus of our study in DS10, where we discussed in detail the appearance of the instability. (The phenomena summarized below can be seen in figs. 4,5 and 6 of that paper.) The instability is characterized by large amplitude outbursts followed by long periods of quiescence in which the accretion rate onto the star drops to zero. The duty cycle for the instability depends on all three parameters ($\Delta r/r_{\rm in}$,$\Delta r_2/r_{\rm in}$,

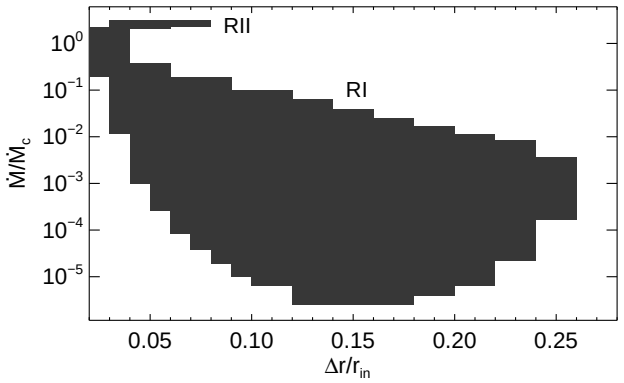

Figure 3. Instability map in $[\dot{m}, \Delta r/r_{\rm in}]$, keeping $\Delta r_2/r_{\rm in} = 0.014$ fixed. The shaded regions denote unstable simulations. The instability occurs in two nearly disconnected regions of the parameter space.In this slice, one (RI) is present over a large range in $\Delta r/r_{\rm in}$ and $\dot{m}$, the other in a small region in $\Delta r/r_{\rm in}$ at $\dot{m} \simeq \dot{m}_{\rm c}$ (RII).

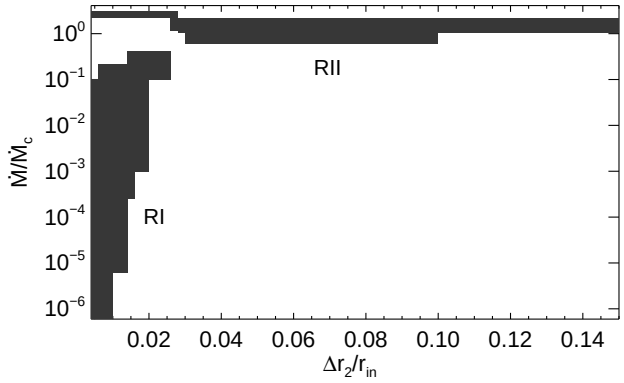

Figure 4. Instability map in $[\dot{m}, \Delta r2/r_{\rm in}]$, keeping $\Delta r/r_{\rm in}$ fixed at 0.05, with shaded areas denoting unstable cases. The two regions of the instability are more clearly separated than in the slice of fig. 3. RI only occurs for very small values of $\Delta r_2/r_{\rm in}$ while RII occurs around $\dot{m} \simeq \dot{m}_{\rm c}$, over a large range in $\Delta r_2/r_{\rm in}$, extending beyond the region of the graph.

and $\dot{m}$), decreasing significantly as the mean accretion rate drops (and mass takes longer to accumulate and power another cycle). The outburst profile generally takes the shape of a relaxation oscillator, with an initial accretion peak followed by a tail of much lower amplitude accretion. Additionally, during the long phase of the outburst suboscillations sometimes appear in the accretion profile. These suboscillations have a much higher frequency than the overall burst, and appear to be the second instability (RII) superimposed on the outburst while the mean acccretion rate onto the star is temporarily higher. As the mean accretion rate is decreased, the outburst becomes shorter and shorter, until finally it simply appears as a single spike of accretion followed by a long period of quiescence.

The second instability region (RII) occurs only around $\dot{m}/\dot{m}_{\rm c} \simeq 1$, in a relatively small range of $\Delta r/r_{\rm in} = [0.01, 0.07]$, but over a large range in $\Delta r_2/r_{\rm in}$. (We have truncated the figure at $\Delta r_2/r_{\rm in}$ to make RI more prominent, but additional simulations show that the instability continues to larger values of $\Delta r_2/r_{\rm in}$, up to at least 0.4). Fig 5 shows four sample simulations for RII taken from the output of our $[\Delta r_2, \dot{m}]$ set of simulations. The simulations all have $\dot{m} = 1.05\ \dot{m}_{\rm c}$ and $\Delta r/r_{\rm in} = 0.05$, with increasing $\Delta r_2/r_{\rm in}$ from bottom to top: $\Delta r_2/r_{\rm in} = [0.028, 0.05, 0.1, 0.15]$. The instability has a different character from the RI instability. The quiescent phase is absent and there is always some accretion onto the star, even during the low phase of the cycle. The shape of the instability is also significantly different from the RI instability: there is no additional higher frequency oscillation, and the outburst profile is smoother. In particular, the initial spike of accretion seen in RI is completely absent. The profile is nearly sinusoidal for small values of $\Delta r_2/r_{\rm in}$ (although the duty-cycle is always less than 0.5). For larger values of $\Delta r_2/r_{\rm in}$, the outburst is characterized by a rapid rise, followed by a decaying plateau and then rapid decline to the low phase of the cycle.

4.2 Period and Amplitude of Instability

We can use our high resolution survey of the instability parameter space to study quantitatively how the properties of the instability change as a function of the different parameters. This allows us to see the differences between the RI and RII instability regions more clearly, and better understand how the instability operates. It also allows us to make more general predictions for the appearance of the instability that can be tested against observations.

To measure the period of the instability we autocorrelate the output of each simulation, and take the first peak in the autocorrelation. All our simulations take as initial conditions the stable solution given by (7) that then becomes unstable. However, the instability generally takes some time to reach a stable period and amplitude, which varies significantly between simulations. This introduces some error in the estimate of the period (particularly in RII, where the instability takes longer to emerge), which is reflected in the figures below.

Figs. 6 and 7 show the instability period [top] and maximum amplitude [bottom] as a function of accretion rate for each unstable simulation in figs. 3 and 4 respectively. Each individual curve represents a different value for $\Delta r/r_{\rm in}$ or $\Delta r_2/r_{\rm in}$, with the colours evolving from purple (smallest parameter value) to red (largest). In the top panels, the gaps in the curves denote stable cases. In the bottom panels, the dashed $y = x$ line shows the mean accretion rate for each simulation.

Some general properties of the period and amplitude of the outburst are valid for both for RI (low $\dot{m}$; cf. sec. 4.1) and RII (high $\dot{m}$). The period of the instability shows an approximately power-law dependence on accretion rate, with an index independent of $\Delta r/r_{\rm in}$ and $\Delta r_2/r_{\rm in}$. It also varies strongly with both $\Delta r/r_{\rm in}$ and $\Delta r_2/r_{\rm in}$. The period scales directly with $\Delta r/r_{\rm in}$. The maximum amplitude of the cycle also scales roughly linearly with $\Delta r/r_{\rm in}$ and$\Delta r_2/r_{\rm in}$. It shows the opposite trend for $\Delta r_2/r_{\rm in}$, decreasing as $\Delta r_2/r_{\rm in}$ increases. On the other hand, the amplitude of the outburst is nearly independent of the mean accretion rate onto the star for a given $\Delta r/r_{\rm in}$ or $\Delta r_2/r_{\rm in}$, as is seen in the bottom panel of figs. 6 and 7. Rather than producing a weaker outburst, at low $\dot{m}$ the duration of the low phase of the outburst increases as mass accumulates in the disc.

This result demonstrates that the details of the outburst, apart from the period of the cycle, are largely independent of $\dot{m}$, and depend almost only on $\Delta r/r_{\rm in}$ and $\Delta r_2/r_{\rm in}$. For large $\Delta r/r_{\rm in}$ a larger reservoir of mass is available for outburst, so that the duration of each burst increases. Smaller $\Delta r_2/r_{\rm in}$ means a more abrupt transition around $r_{\rm c}$ from accreting to non-accreting states, so that for the same $\dot{m}$, a simulation with small $\Delta r_2/r_{\rm in}$ can build up more

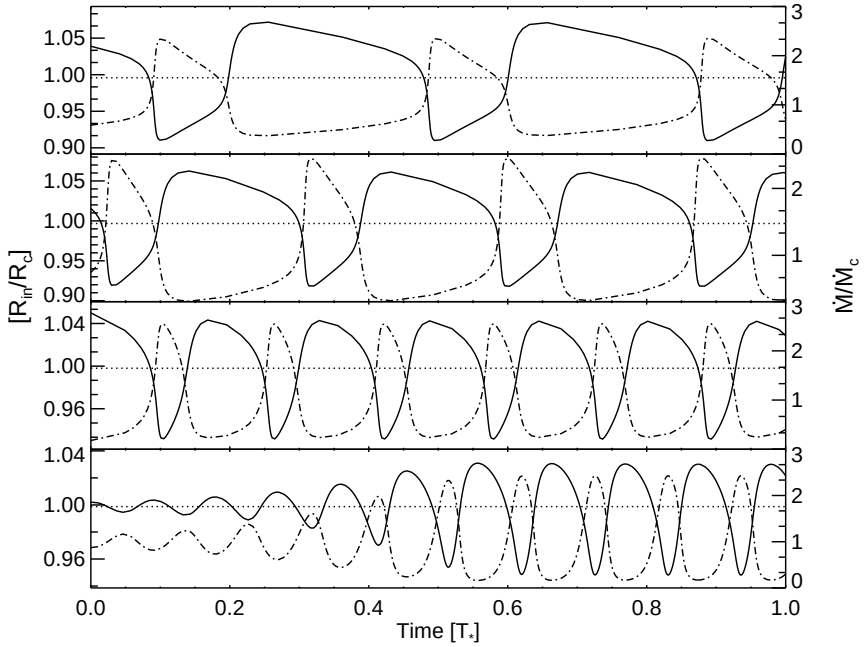

Figure 5. The accretion instability in RII, the second instability region for $\Delta r/r_{\rm in} = 0.05$ and $\dot{m} = 1.05\,\dot{m}_{\rm c}$, with $\Delta r_2/r_{\rm in} = [0.028, 0.05, 0.1, 0.15]$. In each figure, the solid line shows the evolution of $r_{\rm in}$ over a cycle, while the dot-dashed line shows the accretion rate scaled to units of $\dot{m}_{\rm c}$. The dashed line shows the inner radius corresponding to steady-state accretion. The instability only manifests around $\dot{m} \simeq \dot{m}_{\rm c}$, but occurs over a large range in $\Delta r_2/r_{\rm in}$, the transition length between accreting and non-accreting states. Unlike the RI instability, the accretion rate never drops to zero during the quiescent phase of the instability.

mass in quiescence than a simulation with larger $\Delta r_2/r_{\rm in}$, leading to a longer outburst phase and longer period.

Although the trends described above apply to both RI and RII, figs. 6 and 7 clearly demonstrate significant differences between the two regions. In RI the accretion amplitude scales inversely with both $\Delta r/r_{\rm in}$ and $\Delta r_2/r_{\rm in}$, so that a large $\Delta r/r_{\rm in}$ (or $\Delta r_2/r_{\rm in}$) corresponds to an outburst with an amplitude up to $100\times$ smaller than for the same $\dot{m}$ and smaller $\Delta r/r_{\rm in}$ ($\Delta r_2/r_{\rm in}$). The transition between accreting and non-accreting states becomes more gradual as $\Delta r/r_{\rm in}$ ($\Delta r_2/r_{\rm in}$) increase, so it makes sense that the initial peak of the outburst will be lower for larger $\Delta r/r_{\rm in}(\Delta r_2/r_{\rm in})$. Interestingly, the cycle amplitude scales inversely with $\Delta r/r_{\rm in}$, while the period scales directly. The opposite behaviour is true of $\Delta r_2/r_{\rm in}$. Instabilities with large $\Delta r/r_{\rm in}$ thus have weaker outbursts and a longer duty cycle (compared to an instability with smaller $\Delta r/r_{\rm in}$), while those with a large $\Delta r_2/r_{\rm in}$ instead have weaker outbursts and a shorter period, and less variation between outburst and quiescence.

The RII instability is presently not as well-sampled as RI, but some general characteristics are evident. Most significantly, the amplitude is much larger ($\sim 40\%$) than the largest amplitude RI instability, and the period of oscillation is up to $\sim 60\%$ shorter. As well, our present results suggest that the outburst amplitude for RII is roughly *independent* of $\Delta r/r_{\rm in}$, $\Delta r_2/r_{\rm in}$, and $\dot{m}$, staying fixed at about $10\,\dot{m}/\dot{m}_{\rm c}$. Instead of changing in amplitude, as $\langle\dot{m}\rangle$ decreases (or $\Delta r_2/r_{\rm in}$ increases), the period increases as well and the source spends more time in the low phase of the cycle (as is seen in fig. 5).

In summary, the instability is very different in RI and RII. In RI, the period of the instability is 1–1000 times longer than the viscous accretion timescale in the inner parts of the disc, and is a strong function of $\Delta r/r_{\rm in}$, $\Delta r_2/r_{\rm in}$ and $\dot{m}$. The amplitude and duty cycle of the outburst are strong functions of the detailed disc-field interaction around $r_{\rm c}$, but appear nearly independent of $\dot{m}$. The instability occurs over a wide range in $\dot{m}$ and $\Delta r/r_{\rm in}$, but is confined to small values of $\Delta r_2/r_{\rm in}$, the parameter describing the transition from accretion to 'centrifugal barrier'. RII is confined to a small range in $\dot{m}$, but extends to much larger values of $\Delta r_2/r_{\rm in}$. The cycle period is typically shorter than the viscous timescales in the inner disc ($P_{\rm cyc} \sim 10^{-2} - 1\ t_{\rm c}$), and the amplitude of the outburst is higher than RII. The amplitude of the outburst appears to be independent of $\dot{m}$, Δr and Δr_2, with a typical value of $\sim 10\,\dot{m}_{\rm c}$.

4.3 Interpretation of the instability regions

The instability in region I is easiest to understand; it corresponds to the cyclic accretion predicted by Sunyaev & Shakura (1977), and studied in Spruit & Taam (1993). Mass piling up at the centrifugal barrier eventually becomes large enough to 'open the gate', and the resulting accretion rate is large enough to push the inner edge of the disc inside corotation for a while, until the mass reservoir has been drained. Unlike a fixed reservoir, the mass in it is not a fixed number, since it depends on the extent of the disc participating in the cycle. This explains the large range in cycle period over which it operates (Spruit & Taam 1993).

This view of the RI cycle implicitly assumes a sharp transition from accretion to pile-up outside $r_{\rm c}$. If the transition is not sharp and the centrifugal barrier is 'leaky', the cyclic behavior can be avoided. Mass still piles up outside $r_{\rm c}$, but accretion can be matched by mass leaking through the barrier. This explains why the cycles are limited to low values of $\Delta r_2/r_{\rm in}$. As in Spruit & Taam (1993), the cycles can start from a steady accreting state in the form a linear instability, which sets in only if the transition is steep enough.

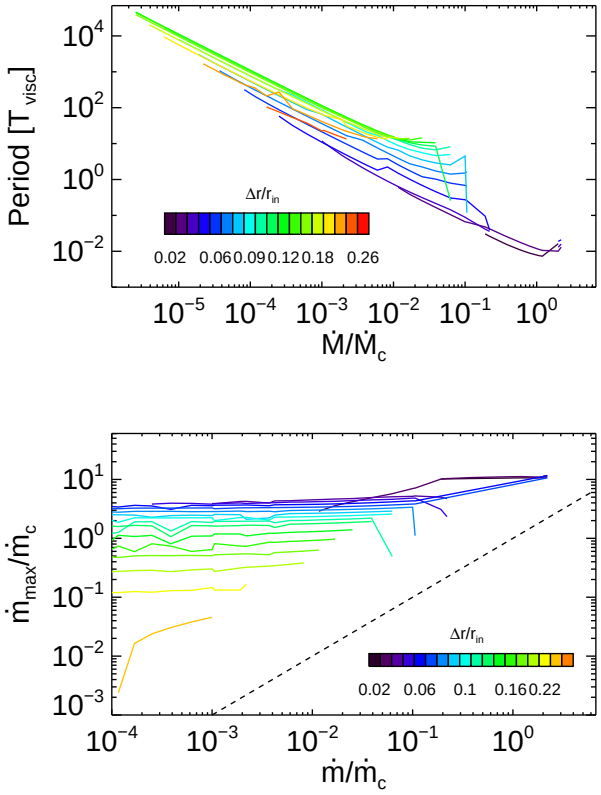

Figure 6. Period [top] and amplitude [bottom] of the instability as a function of $\dot{m}/\dot{m}_{\rm c}$ for the unstable simulations shown in fig. 3. The accretion rate spans the range $\dot{m} = [10^{-6}, 6]$ and $\Delta r/r_{\rm in} = [0.02, 0.28]$. The individual curves show differen values of $\Delta r/r_{\rm in}$, increasing from black (smallest) to red (largest). In the top panel, the gaps in the curves indicate regions of stable accretion. In the bottom panel, the mean accretion rate is indicated by the dashed $y = x$ line.

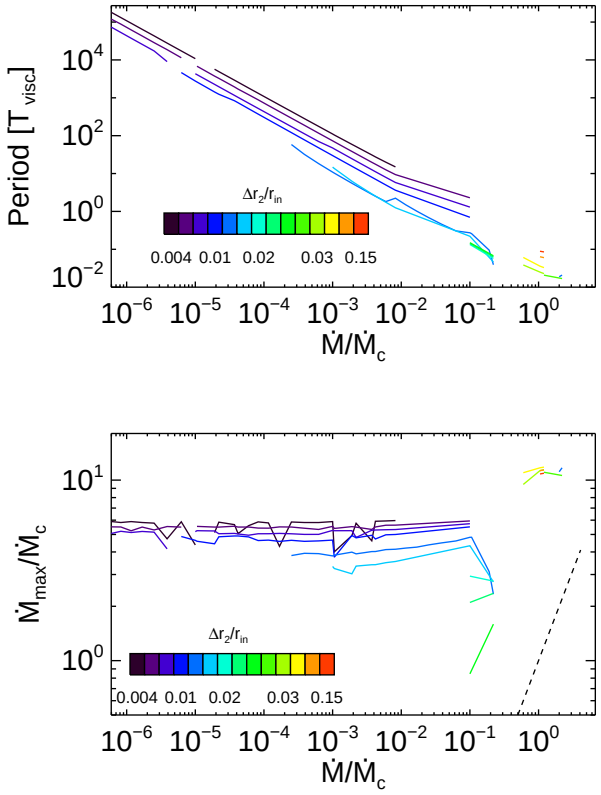

Figure 7. Period [top] and amplitude [bottom] of the instability as a function of $\dot{m}/\dot{m}_{\rm c}$ for the simulations shown in fig. 4. The plot is the same as fig. 6, replacing $\Delta r/r_{\rm in}$ with $\Delta r_2/r_{\rm in}$. Each curve shows a different $\Delta r_2/r_{\rm in}$ spanning the range $\Delta r_2/r_{\rm in} = [0.004, 0.15]$.

Region II is restricted to accretion rates around the transition to steady accretion , and small values of $\Delta r/r_{\rm in}$. Its restricted range of oscillation periods – a fraction the viscous time scale at $r_{\rm c}$ – shows that it operates on a region of finite extent, of the order of the width of the transitions $\Delta r/r_{\rm in}$, $\Delta r_2/r_{\rm in}$. In the transition region, a small increase in accretion rate will cause $r_{\rm in}$ to move inwards, which will substantially decrease the torque at $r_{\rm in}$ (because $\Delta r/r_{\rm in}$ is small) and moves $r_{\rm in}$ even further inward. As $r_{\rm in}$ moves inward the accretion rate through $r_{\rm in}$ increases and an outburst is triggered. Since even in the low phase of the cycle material is accreted onto the star, the reservoir of matter available for the outburst is small and only the innermost regions of the disc are involved in the instability (of order $\Delta r_2/r_{\rm in}$). The timescale for the instability is thus much shorter than the RI instability, and the period scales with $\Delta r_2/r_{\rm in}$.

Since the instability occurs over a small region around $r_{\rm c}$, it is likely sensitive to the details of the physics of the transition region. As long as we may assume the transition to be monotonic, however, it's shape is rather constrained by its values far from corotation (0 and 1 respectively), and its slope at corotation, (controlled by the width parameter, Δr_2). While the results above show that the existence and properties of the cycle depend strongly on Δr_2, one might wonder to what extent the results also depend on remaining degrees of freedom in the choice of transition function. To test this, we re-ran a series of simulations using the error function rather than the $\tanh -$ function. Since the width of the function is a matter of definition in both cases, we use slope of the function at corotation as a well-defined measure of width for the case-by case comparison. The range of unstable values in the parameter space, the period, shape, and amplitude of the cycle were then found to be very similar as when using a $\tanh$ profile.

4.4 The effect of cycles on angular momentum exchange

The accretion instability can have a significant effect on the spin change with the star. When accretion is stable, the rate of angular momentum exchange between the star and the disc is given by (16), and illustrated in fig. 2. When accretion proceeds via cycles, the amplitude of the outburst is generally much higher than the mean $\dot{m}$, and the disc spends a significant amount of time in the low phase of the cycle, in which little or no accretion takes place (sec. 4.2). This will affect the net angular momentum exchange between the star and the disc: since the low phase of the instability almost always lasts longer than the outburst phase, the star will spin down faster than if accretion proceeded steadily.

Using the results of the simulations presented in sec. 4.1 and 4.2, we can compare the torque exerted on the star for stable and unstable accretion:

$$\frac{\Delta j}{j_{\rm cons}} \equiv \frac{\langle j_{\rm sim}\rangle - j_{\rm cons}}{j_{\rm cons}}. \qquad (17)$$

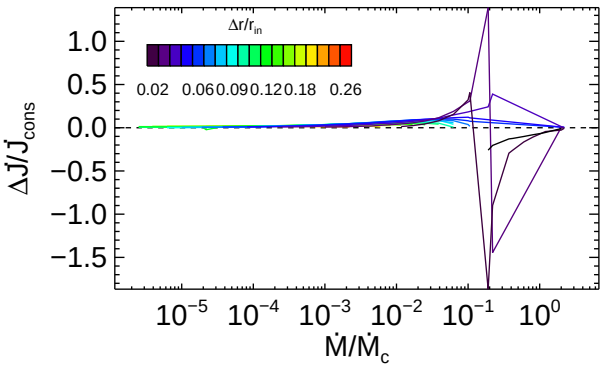

Figure 8. Effect of cycles on the average torque, as a function of accretion rate. Figure shows the difference between the torque in the unstable initial state before the cycle develops, and the value measured in the fully developed limit cycle. The different curves represent different $\Delta r/r_{\rm in}$, increasing from purple ($\Delta r = 0.05$) to red ($\Delta r = 0.22$). $\Delta r_2 = 0.014$ is held constant. Cases that do not become cyclic lie on the red line along the x-axis.

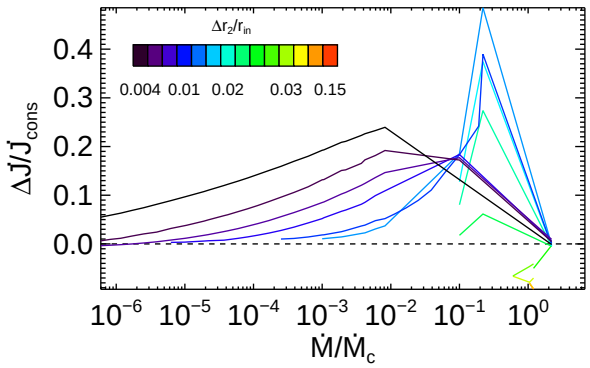

Figure 9. Difference between the torque in the unstable initial state before the cycle develops, and the value measured in the fully developed limit cycle. The different curves represent different $\Delta r_2/r_{\rm in}$, increasing from purple ($\Delta r_2 = 0.004$) to red ($\Delta r = 0.028$). $\Delta r = 0.05$ is held constant. Solutions that lie along the x-axis do not show cyclic variations.

Here $\dot{J}_{\rm cons}$ is the torque exerted on the star in the initial state (calculated using 16), and $\langle \dot{J}_{\rm sim} \rangle$ is the average torque exerted over one full cycle once a stable limit cycle is reached.

Figs. 8 and 9 show $\Delta\dot{J}/\dot{J}_{\rm cons}$ as a function of accretion rate for the simulations in figs. 3 (varying $\Delta r/r_{\rm in}$) and 4 (varying $\Delta r_2/r_{\rm in}$), respectively. The individual curves show different $\Delta r/r_{\rm in}$ (or $\Delta r_2/r_{\rm in}$), with the colours from purple to red indicating increasing values of the parameter. Lines along the x-axis are stable solutions.

The results are easily separated into the RI (low $\dot{m}$) and RII (high $\dot{m}$) instability regions. In RI, both $\dot{J}_{\rm cons}$ and $\dot{J}_{\rm sim}$ are negative (cf. 2) over the entire unstable region, and the star spins down. As expected, the presence of the instability increases the efficiency of the spin-down torque considerably: by up to 50% for $[\Delta r/r_{\rm in}, \Delta r_2/r_{\rm in}] = [0.05, 0.015]$. For a given value of $\Delta r/r_{\rm in}$ or $\Delta r_2/r_{\rm in}$, $\Delta\dot{J}/\dot{J}_{\rm cons}$ is largest at the highest $\dot{m}$ and decreases for smaller $\dot{m}$. When $\dot{m}$ stays fixed, $\Delta\dot{J}/\dot{J}_{\rm cons}$ is largest for the smallest values of $\Delta r/r_{\rm in}$ and $\Delta r_2/r_{\rm in}$ (where the outburst amplitude is largest, cf. sec. 4.2). This behaviour is readily understandable: the added angular momentum from accretion is most relevant at high $\dot{m}$, and the rate at which this material is accreted (i.e. the duty cycle of the outburst) will determine how much the star will spin up or down. The larger the amplitude of the outburst, the faster the reservoir of mass will be accreted, and so the shorter the duty cycle.

In RII the situation is quite different. In the parameter range for $\Delta r/r_{\rm in}$ and $\Delta r_2/r_{\rm in}$ where the solution is unstable, $\langle \dot{J}_{\rm sim} \rangle$ and $\dot{J}_{\rm cons} > 0$ when $\dot{m} = \dot{m}_{\rm c}$ (fig. 2). The presence of the instability decreases the rate of spin-up by a maximum by up to about 10%.

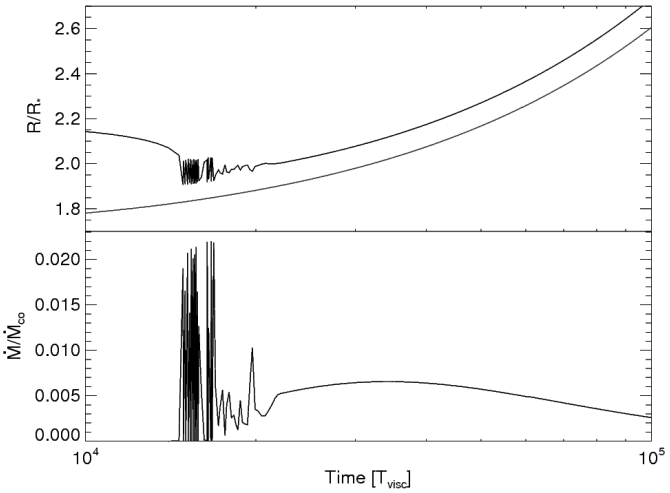

Figure 10. Unstable disc solution for $[\Delta r, \Delta r_2] = [0.2, 0.02] r_{\rm in}$. At $t = 0$, $r_{\rm in}/r_{\rm c} = 1.3$, so that $\dot{m} \simeq 0$. Initially $r_{\rm in}$ remains constant, before decreasing sharply as $r_{\rm c}$ increases. This prompts the onset of the accretion instability, which continues even while the star spins down. At later times, the amplitude and frequency of the instability decrease and the disc reverts back to accreting steadily. Top: Evolution in $r_{\rm in}$ (black curve) and $r_{\rm c}$ (red curve), before, during, and after the instability appears. Bottom: Corresponding accretion rate onto the star. The accretion rate is given in terms of $\dot{m}_{\rm c}$ corresponding to $r_{\rm c}$ at $(t = 0)$.

4.5 Transient instability cycles

In DS11 we studied how discs in our model evolved as the spin of the star changed. To do this we introduced the star's moment of inertia, I_* as an additional parameter of the problem, which introduced a new characteristic timescale for the problem, the spindown timescale $T_{\rm SD}$:

$$T_{\rm SD} \equiv P_*/\dot{P}_* \sim \frac{I_* \Omega_* r_{\rm in}^4}{\eta \mu^2 \Delta r}. \qquad (18)$$

We found that the ratio of $T_{\rm visc}$, the viscous accretion timescale at $r_{\rm c}$, and $T_{\rm SD}$ plays an important role in determining whether a disc will become trapped with $r_{\rm in}$ close to $r_{\rm c}$ when $\dot{m}$, the mean accretion rate through the disc drops to zero.

The spin change of the star can also determine whether or not the accretion instability occurs. For a given set of $[\Delta r, \Delta r_2]$ the instability frequently appears over a narrow range in $\dot{m}/\dot{m}_{\rm c}$, so that changing $r_{\rm c}$ (and hence $\dot{m}_{\rm c}$) will cause the instability to appear or disappear. This effect is difficult to observe in our simulations, since the timescale of the instability ($\sim 10^{-2} - 10^3\ T_{\rm visc}$) is in general much shorter than the spin-down timescale of the star ($T_{\rm SD} \sim 10^3 - 10^{17}\ T_{\rm visc}$; DS11), so once the instability occurs the simulation typically proceeds on the instability timescale. Despite

this, we do find some solutions that show transient oscillations (typically those with the long periods, $P \sim 10^3 T_{\rm visc}$) for a constant $\dot{m}$, which appear and disappear as $r_{\rm c}$ changes.

This transient instability is illustrated in figs. 10 and 11. For these simulations we have adopted the same scaling parameters as we used in DS11. We take r_*, the star's radius, as our characteristic length scale, and define $t_* \equiv \nu/r_*^2$, the nominal viscous timescale at the star's radius, as the characteristic timescale. We set $T_{\rm SD} \equiv 380\, T_{\rm visc}$ (where $T_{\rm visc}$ is the viscous timescale for $r_{\rm c}(t=0)$), which is appropriate for a protostellar system. We set $r_{\rm c}(t=0) = 1.8 r_*$.

In fig. 10 we show the evolution of an initially dead disc ($\dot{m} = 0$) with $[\Delta r/r_{\rm in}, \Delta r_2/r_{\rm in}] = [0.2, 0.02]$. The disc is initially in the steady-state solution given by (7) with $r_{\rm in} = 1.3 r_{\rm c}$. The top panel shows the evolution of $r_{\rm in}$ (black) and $r_{\rm c}$ (red) in time, while the bottom panel shows the accretion rate onto the star, scaled to $m_{\rm c}$ at $t = 0$. At early times [not shown] there is no accretion onto the star and $r_{\rm in}$ remains fixed while $r_{\rm c}$ moves steadily outwards. Once $r_{\rm c}$ moves close enough to $r_{\rm in}$ (at $\sim 10^4 t_*$) to begin accreting matter, gradients in the disc's surface density cause $r_{\rm in}$ to move quickly closer to $r_{\rm c}$. At $r_{\rm in}/r_{\rm c} \sim 1.1$, however, the disc suddenly becomes unstable and accretion proceeds via a series of large amplitude bursts, which increase the maximum accretion rate onto the star enormously. $r_{\rm c}$ continues to move outwards as the source oscillates, which causes $\dot{m}_{\rm c}(r_{\rm c})$ to decrease as well. Eventually $\dot{m}/\dot{m}_{\rm c}$ moves out of the unstable range, and the disc settles back into a steadily accreting solution with a gradually decreasing accretion rate. This result emphasizes the fact the instability can depend sensitively on $\dot{m}/\dot{m}_{\rm c}$, so that as $r_{\rm c}$ evolves, cycles can appear and then disappear.

For constant $\Delta r/r_{\rm in}$ and $\Delta r_2/r_{\rm in}$, the appearance of cycles depends on $\dot{m}$ and $\dot{m}_{\rm c}$. As we showed in DS11, when the mean accretion rate through the disc drops so low that the disc becomes trapped, the accretion rate at $r_{\rm in}$ depends strongly on $T_{\rm visc}/T_{\rm SD}$. This ratio also plays an important role in determining the presence and duration of unstable accretion phases.

We illustrate this in fig. 11, which shows a disc evolving from an accreting disc to a trapped disc for different $T_{\rm visc}/T_{\rm SD}$, adopting parameters appropriate for a neutron star. We take the field strength 10^{12} G, initial spin period 5s, and initial inner edge radius $0.95 r_{\rm c}$. The disc is thus initially in an accreting state. The outer boundary is located at $100\ r_{\rm in}$. The initial spindown timescale of the star is $T_{\rm SD} = 10^5$ years. We adopt the same system parameters as for fig. 10, with $[\Delta r/r_{\rm in}, \Delta r_2/r_{\rm in}] = [0.2, 0.02]$. At $t = 0$ we set $\dot{m} = 0$ at the outer boundary of the disc, so that the accretion rate through the disc gradually drops.

The figure shows the evolution of $r_{\rm c}$ (dashed curve) and $r_{\rm in}$ (solid curve) as a function of time for increasing $T_{\rm visc}$, with $T_{\rm visc}/T_{\rm SD} = 2.5 \times [10^{-9}, 10^{-7}, 10^{-5}, 10^{-4}]$ from top to bottom. In all four simulations, the disc initially move outwards as $\dot{m}$ decreases to about $1.05\, r_{\rm c}$, where the accretion rate triggers the onset of the instability.

The appearance of the disc changes dramatically with changing viscosity. Discs with a high viscosity are able to diffuse outwards quickly as $\dot{m}$ declines, so that $r_{\rm in}$ in the top panel (with the highest viscosity) moves far from $r_{\rm c}$ before the star can begin to spin down, and the disc never becomes trapped close to $r_{\rm c}$. The instability (which only occurs between $\dot{m}/\dot{m}_{\rm c} \simeq [10^{-3}, 0.1]$) will only appear briefly before $r_{\rm in}$ moves too far from $r_{\rm c}$ and the accretion rate drops. In the middle two panels the instability also appears briefly, but the star does begin to spin down quickly enough that $r_{\rm c}$ begins to move outwards at the same rate as $r_{\rm in}$ and the disc remains trapped. In the bottom panel (with the lowest viscosity), the disc diffuses outwards slowly, and the star spins down more rapidly. Once the instability is triggered, $r_{\rm in}$ remains close enough to $r_{\rm c}$ that the instability persists as the star continues to spin down.

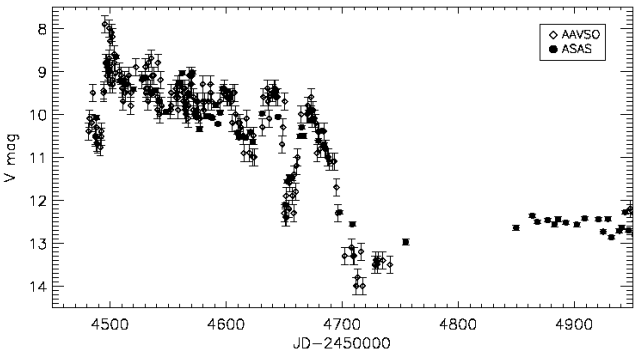

Figure 12. The 2008 outburst of EX Lupi. From January to August, the source was up to 4 magnitudes larger than its quiescent value. *Figure courtesy A. Juhasz.*

5 RELEVANCE FOR ASTROPHYSICAL SOURCES

5.1 Trapped discs and the disc instability in EXors

We have previously suggested that the disc instability discussed in this paper is operating in a class of T Tauri stars known as 'EXors'. EXors, like their prototype, EX Lupi are characterized by repeated large outbursts: changes by up to four magnitudes in luminosity lasting several months, with a characteristic total period of several years (Herbig 2007, 2008). Observations of these sources in both outburst and quiescence can produce valuable constraints on both the disc instability and the trapped disc itself.

Figure 12 shows the $m_{\rm V}$ brightness of EX Lupi over 500 days, taken from the AAVSO and ASAS archives (from Attila Juhasz, *private communication*). In January 2008, EX Lupi underwent a large outburst, increasing by 3 magnitudes, from $m_{\rm V} = 11$ to $m_{\rm V} = 7.9$ (Aspin et al. 2010) in about 20 days. In July 2008 EX Lupi was at $m_{\rm V} = 12.4$ (Sipos et al. 2009), so the total change in luminosity was more than 4 magnitudes. EX Lupi remained in outburst for eight months, decaying from maximum to about $m_{\rm V} = 10$ before abruptly dropping to $m_{\rm V} = 14$ over about 40 days. The data show evidence of an additional higher-frequency modulation with a period of about 30 days and amplitude of 1-2 magnitudes.

The outburst profile looks similar to some of the profiles seen in our simulations, with a rapid rise and a gradual decreasing plateau phase, followed by a rapid decay as the source returns to quiescence. The higher frequency modulation is also suggestive of the higher frequency oscillations seen in the RI instability discussed above and in DS10, although its short timescale $\sim$ 30 days, or $\sim 4 - 10\times$ longer than P_* (Sipos et al. 2009) might also indicate direct modulation between the disc and magnetic field (e.g. Goodson, Winglee & Boehm 1997; Romanova, Kulkarni & Lovelace 2008).

Spectral observations taken both during the outburst and quiescence allow additional constraints on the disc model. Aspin et al.

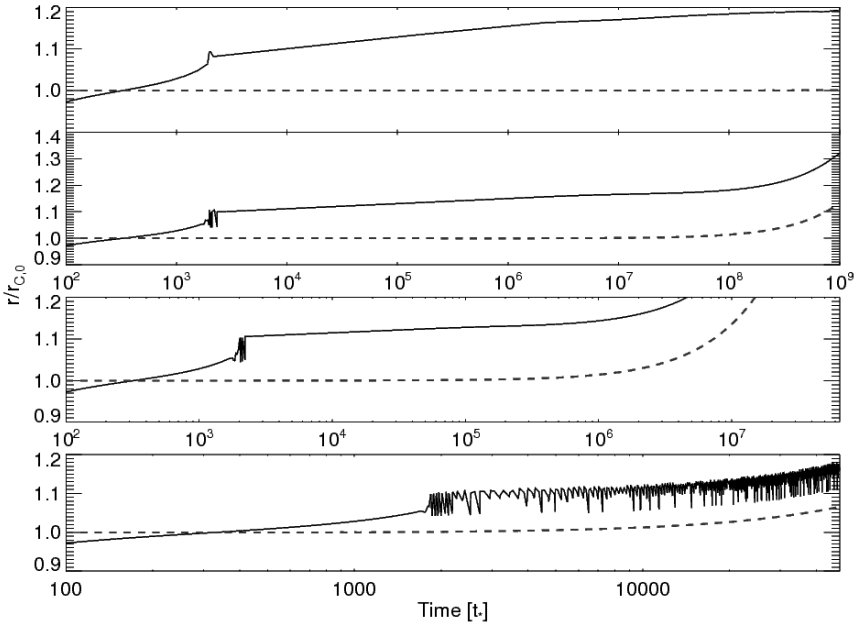

Figure 11. Evolution from an accreting to a non-accreting disc, for increasing (top to bottom) ratios of $T_{\rm visc}/T_{\rm SD}$ for stable discs ($\Delta r/r_{\rm in} = 0.1$, $\Delta r_2/r_{\rm in} = 0.04$). From top to bottom, the ratio $T_{\rm visc}/T_{\rm SD}$ is $2.5 \times [10^{-9}, 10^{-7}, 10^{-5}, 10^{-4}]$. The instability appears in all four panels, for varying lengths of time. As the ratio between the two timescales decreases, the disc is not able to move outwards as quickly before the star begins to spin down, so that $r_{\rm in}$ will always remain close to $r_{\rm c}$ and the instability persists for longer.

(2010) analysed a series of spectra of EX Lupi from the 2008 outburst to constrain the parameters of the disc. They calculated an accretion rate of $2 \times 10^{-7} M_{\odot}{\rm yr}^{-1}$ in outburst, and modelled the 2.2935μm CO overtone emission to suggest an inner gap of about 10 r_* in the disc. They also used previously published results to calculate $6 \times 10^{-9} M_{\odot}{\rm yr}^{-1}$ for the quiescent emission. Sipos et al. (2009) analysed a series of spectra for EX Lupi in quiescence (with $m_{\rm V} \sim 12$), and did a detailed fit for the spectrum. They estimated an accretion rate of $4 \times 10^{-10} M_{\odot}{\rm yr}^{-1}$, and fit the spectrum with a dust-dominated disc truncated at about 0.2 AU. These observations thus suggest that the accretion rate increased by $\sim 30 - 500\times$ during the outburst, and that close to the star, gas is either absent or optically thin.

To see whether these observations are compatible with our model of a trapped disc, we adopt the best-fit parameters of Sipos et al. (2009), with $M_* = 0.6 M_{\odot}$, $r_* = 1.6 R_{\odot}$, and $P_* = 6.3d$ (based on $v \sin i = 4.4 km/s$ and an inclination of 20 degrees). The magnetic field is unknown, so we assume a strong dipolar field with $B_* = 1500G$, which is comparable to field strengths observed in T Tauri stars such as BP Tau (Donati et al. 2008). The rest of the parameters we adopt are the same as for our representative model (sec. 2.1). This puts the co-rotation radius at 7.6 r_*, and sets $r_{\rm in} \simeq r_{\rm c}$ for the quiescent disc. The viscous timescale at $r_{\rm c}$ is thus ~ 30 yrs. If we assume that the period of the instability is $\sim$ 60 yrs (the time between the 2008 outburst and the similar amplitude outburst in 1955), or $\sim T_{\rm visc}$. The instability would then fall in the RII region.

Additional information could come from directly detecting the accretion disc itself in quiescence. A trapped disc will have both a higher surface density and temperature than a standard accreting disc with the same $r_{\rm in}$. For EX Lupi in quiescence (using the parameters given above), our model predicts a surface temperature from internal viscous dissipation of 530-650K (depending on $\dot{m}$), compared with 290-570K for a Shakura-Sunyaev disc. This modest temperature increase is likely insignificant compared to heating from the central star, which will thus still determine the gas behaviour at these low accretion rates (e.g. Muzerolle et al. 2004). The surface density in the disc will also increase modestly, from a maximum of between 3-40 g cm^{-2} ($\rho \simeq 4 \times 10^{-11} - 6 \times 10^{-10}$ g cm^{-3} to 40-80 g cm^{-2} ($\rho \simeq 4 \times 10^{-10} - 10^{-9}$ g cm^{-3}). At these low densities the disc is probably optically thin (e.g. Dullemond & Monnier 2010), so that it is likely not possible to directly distinguish between a trapped disc and normal accreting one except through detailed modelling of spectral features in the disc.

Unlike the accretion instability (which only occurs under certain conditions in the disc-field interaction), the build-up of mass just outside the co-rotation radius should be generic in stars with strong magnetic fields and relatively low accretion rates. The best opportunity to detect a trapped disc directly would come from a star with a strong dipolar magnetic field, high spin rate and low accretion rate, so that the disc would be optically thick rather than thin (as would be expected for the given accretion rate), and could be directly detected through modelling of its spectral features.

5.2 NS transients w/ weak recurrent outbursts

In DS11 we suggested that the large ratio between the spin-down and viscous timescales in accreting millisecond pulsars makes it unlikely that the disc will become trapped, since as $\dot{m}$ drops $r_{\rm in}$ moves outwards much faster than $r_{\rm c}$. This agrees with the typical outbursts seen in transient X-ray pulsars, which show outbursts of variable duration followed by long periods of quiescence and are believed to be triggered by ionization instabilities in the disc (e.g. Lasota 2001).

However at least two accreting X-ray pulsars, NGC 6440 X-2 (Heinke et al. 2010) and IGR J00291+5934

(Hartman, Galloway & Chakrabarty 2010) have been observed to undergo weak, recurrent outbursts on much shorter timescales (around 30 days) than would be predicted from an ionization-instability model (Lasota 2001). The weakness of the outburst has been interpreted to mean that the disc is never completely ionized during the outburst Hartman, Galloway & Chakrabarty (2010), which suggests the ratio of $T_{\rm SD}/T_{\rm visc}$ becomes small enough to trap the disc as when the accretion rate drops. This large reservoir of matter would then be present when the accretion rate again increases, and so could allow more frequent outbursts. These sources thus offer an excellent opportunity for comparison with our model of a trapped disc.

IGR J00291+5934 is a 599Hz X-ray pulsar in a 147 minute orbit, which historically has shown standard single outbursts (in 1998, 2001, and 2004) followed by long periods of quiescence. However, in 2008 it underwent a substantially different outburst, with two weaker outbursts (respectively lasting nine and 13 days) separated by 27 days of quiescence (Hartman, Galloway & Chakrabarty 2010). The authors estimated that the total mass flux of weaker outbursts together was approximately equal to the single 2004 outburst. Similar outbursts have been seen in NGC 6440 X-2, a recently discovered X-ray binary with a frequency of 442Hz in a 57 minute orbit (Altamirano et al. 2010). Since discovery on July 28, 2009, five distinct outbursts have been observed, each typically lasting around four days at a luminosity of around $L_X \sim 10^{35}{\rm erg\ s^{-1}}$, with a minimum recurrence time of around 31 days.

The short recurrence timescales suggest that a considerable amount of mass is stored in the disc when the accretion rate drops, which can then fuel another outburst when $\dot{m}$ increases again. In both sources the quiescent X-ray luminosity is at least 4 orders of magnitude lower than the outburst luminosity, indicating a large change in accretion rate (although the X-ray luminosity may not be a good indicator of bolometric luminosity at such low accretion rates, so there is some uncertainty in the change in $\dot{m}$).

During two outbursts, the power spectrum of NGC 6440 X-2 was dominated by a strong low-frequency QPO ($\sim$ 1 Hz) (Patruno et al. 2010; Hartman, Galloway & Chakrabarty 2010). A similar QPO was previsouly detected in the tail an outburst in X-ray pulsar SAX J1808.4-3658 (Patruno et al. 2009) which was attributed to the disc instability presented in DS10 and Spruit & Taam (1993). A much weaker QPO at 0.5 Hz was observed in the outbursts IGR J00291+5934 and might also be attributed to the disc instability (Hartman, Galloway & Chakrabarty 2010).

The fact that all of these QPOs were observed at a similar frequency presents a challenge to our interpretation. The outbursts seen in SAX J1808.8-3658 follow the more conventional pattern of a large outburst followed by a long quiescence, which would suggest that a dead disc does not form. However, the similarity of the QPO frequency (which is roughly correlated with the viscous timescale near $r_{\rm in}$ in our model) suggests that the viscous timescale is similar in all these sources. This contrasts with our suggestion that the viscosity in these weak outbursts is substantially smaller than in larger outbursts. The number of uncertain parameters in our model (in particular this assumes that $\Delta r_2/r_{\rm in}$ is similar in all sources) means that the picture we have presented could still be valid, but then the similarity in QPO frequency in both (or all three) of these sources is probably coincidental. On the other hand, a strong low-frequency QPO has currently been observed in only two sources, while as Altamirano et al. (2010) have noted, weakly outbursting sources like NGC 6440 X-2 will generally be missed in current surveys.

In our present model, the disc-field interaction is not responsible for directly regulating the accretion rate onto the star to control the outbursts, as was suggested by Hartman, Galloway & Chakrabarty (2010). The field can temporarily halt accretion onto the star, but only on the much shorter timescale on which the 1Hz QPO is seen. Thus the mechanism that directly triggers an accretion outburst remains undetermined.

5.3 Persistent X-ray pulsars

A small subset of accreting pulsars with low-mass companions have sufficiently persistent X-ray emission to measure the spin change directly and study the connection between spin change and luminosity. Three well-studied persistent sources (Her X-1, 4U 1626-67, and GX 1+4) all show episodes of spin-up and spin-down, although the pattern of spin-up and spin-down is different in all three (Bildsten et al. 1997). A fourth, (GRO J1744-28) shows clear spin-up when in outburst, allowing the relationship between $\dot{\nu}$ and $\dot{m}$ to be constrained.

The binary properties of all these sources varies considerably, both in their companions and orbital periods. However, it is still possible to make some general observations that apply to all sources. First, there is a clear correlation between luminosity and spin change, with higher luminosity corresponding to spin up, and vice versa. Second, when the star is spinning up, the spin-up rate is substantially lower than would be predicted from the X-ray luminosity. Third, where the relationship between $\dot{\nu}$ and $\dot{m}$ can be measured, $\dot{\nu} \propto \dot{m}^{\gamma}$, where $\gamma > 6/7$, i.e. the scaling expected for $r_{\rm in} \propto \dot{m}^{-2/7}$. Finally, the spin-up torque is often comparable (within a factor 2) to the spin-down torque, with only a change in sign.

The first observation is universally expected in magnetospheric accretion, since in order to spin up the star the matter must be able to overcome the centrifugal barrier imposed at $r_{\rm c}$. The second point is also readily understandable in our model, which assumes that there is a transition region for $r_{\rm in} \sim r_{\rm c}$ in which there is both accretion and spin-down torque. This behaviour is also seen in MHD simulations of the disc-star interaction (e.g. Romanova et al. 2004). For high accretion rates, our model predicts $\dot{\nu} \propto \dot{m}^{9/10}$, which is close to the dependence measured in some X-ray pulsars in outburst. For example, the 1995/1996 outburst of GRO J1744-28 (a disc-fed binary), was measured to follow $\dot{\nu} \propto \dot{m}^{0.96}$ (Bildsten et al. 1997). This is closer to observation than the standard model, which predicts an index of $6/7$.

The final point is most puzzling in a model in which $r_{\rm in} \propto \dot{m}^{-2/7}$, because it requires that the change in accretion rate is finely tuned to preserve this symmetry. It is more plausible for our model, however, which shows a steep decrease in $\dot{\nu}$ around $\dot{m}/\dot{m}_{\rm c} = 1$, and then a flattening around the minimum in $\dot{\nu}$. Thus, a small decrease in $\dot{m}$ will cause an initial steep transition to spin-down before settling around the minimum in $\dot{\nu}$. There is no comparable turnover at high $\dot{m}$, but in order to switch between spin-up and spin-down, the star must have an average accretion rate such that $r_{\rm in} \sim r_{\rm c}$, while in order to be a persistent source, the accretion rate at large distances cannot be very variable. If we assume that the average accretion rate has been steady enough on long timescales to affect the star's rotation rate, then there will be a natural spin-down torque, set by the minimum in 2, and we would expect that on average the accretion rate would fluctuate around the level that keeps $r_{\rm in}$ close to $r_{\rm c}$. This still does not account for the observations (for example of 4U 1626-27) in which the magnitude of the torque is very nearly symmetric.

Our present model is too simple to make quantitative com-

parisons to data. For one thing, the relation between $\dot{\nu}$ and $\dot{m}$ depends on the least certain parts of our model: both the transition widths $\Delta r/r_{\rm in}$ and $\Delta r_2/r_{\rm in}$ and the connecting functions y_m and y_Σ. There is also much more variation in the luminosity at which the system moves from spin-up to spin-down than is generically predicted in any simple magnetospheric accretion model. This variability could indicate fluctuations in $\langle\eta\rangle$, and $\Delta r/r_{\rm in}$, which would both affect the magnitude of spin-down torque. Agapitou & Papaloizou (2000) demonstrated that the value of B_ϕ changes if field lines are able to diffuse radially through the disc. The diffusion of field lines is expected to happen on viscous timescales (Fromang & Stone 2009), so that the details of the disc-field interaction could in fact rely on the complicated interplay between the accretion rate and the field strength and geometry. Such questions require detailed MHD modelling which are beyond the scope of the present work.

6 DISCUSSION

At low accretion rates, the strong magnetic field of a star can strongly alter the structure of an accretion disc, preventing it from either accreting or expelling material outward, and preventing the inner edge of the disc from moving considerably away from $r_{\rm c}$. As we have discussed in this paper, this disc state can lead to substantially different behaviour from what is conventionally assumed, and could explain a variety of observed phenomena in magnetically accreting stars. However, in order to construct our model we used a parameterized description for the interaction between the magnetic field, introducing the free parameters $\Delta r/r_{\rm in}$, and $\Delta r_2/r_{\rm in}$. Here we discuss what sets the value of these parameters, and whether these parameters could vary in time, which could account for some of the additional behaviour not described by our current model.

The first parameter, $\Delta r/r_{\rm in}$ is the width of the direct interaction between the field and the disc in the disc's innermost region. We have assumed in all cases that $\Delta r/r_{\rm in} < 1$, so that the interaction region (where the field lines remain closed long enough to exert a significant stress on the disc) remains fixed. MHD simulations suggest that this region will fluctuate in time as field lines open and reconnect, but we have assumed that this will occur on timescales of $\sim P_*$, which are much shorter than the viscous timescale of the instability ($T_{\rm visc} > 10^3 P_*$). Numerical MHD simulations do sometimes show variability on longer timescales (e.g. Romanova et al. (2009)), which could lead to changes in $\Delta r/r_{\rm in}$ between individual outbursts. Given that even small changes in $\Delta r/r_{\rm in}$ can significantly change the appearance and amplitude of the outburst (seen in figure 6), variability in the disc-field interaction could produce variability in the appearance of the instability, especially if the instability occurs in RII.

A second possible source of variability could come from the radial evolution of the magnetic field itself. This was studied by (Agapitou & Papaloizou 2000), who found that radial field-line diffusion through the disc can reduce the effective torque at $r_{\rm in}$, and increase the extent of the closed-field line region. The timescale for magnetic diffusion is typically assumed to be about the same as for viscous diffusion (which is supported by recent MRI calcuations; Fromang & Stone 2009), so that the radial diffusion of closed field-lines outward could compete with accretion of matter (and field lines) inward, creating an additional, longer timescale source of variability in $\Delta r/r_{\rm in}$. This could allow the instability to appear and disappear at the same $\dot{m}$ (as has been seen in Patruno et al. 2009, where the 1-Hz QPO was seen in portions of the outburst but not others at the same flux).

The physics that sets $\Delta r_2/r_{\rm in}$ (the transition length between the accreting and non-accreting solutions) is considerably less clear, although presumably the same variations in the disc-field interaction that change $\Delta r/r_{\rm in}$ could also change $\Delta r_2/r_{\rm in}$. In DS11 we discussed the model proposed by Perna, Bozzo & Stella (2006), which considers a strongly inclined dipole, so that the disc truncation radius lies both inside and outside $r_{\rm c}$, allowing for simultaneous accretion and confinement of material. If this is the case then $\Delta r_2/r_{\rm in}$ should remain constant for a given system, and the variability must come from fluctuations in $\Delta r/r_{\rm in}$.

Another open question remains what regulates the mean accretion rate onto the star. In all our simulations we have treated the accretion rate, $\dot{m}$ as a free parameter, and shown how the instability and spin-evolution of the star change as a result. However, observations of neutron star binaries suggest that the accretion rate from the donor star remains roughly constant Bildsten et al. (1997), and variations in $\dot{m}$ are often assumed to arise from ionization instabilities (Lasota 2001). Hartman, Galloway & Chakrabarty (2010) suggested that the disc-field interaction could regulate the accretion rate onto the star by storing it up, in a similar way to what we have discussed here. However, our model does not agree with this conclusion: the disc-field interaction can only halt accretion long enough to build up mass to drive the disc instability and only substantially alters the inner regions of the disc. Our trapped disc solutions evolve *as a response* to the decreased accretion rate in the disc, and only become relevant once the average accretion rate has decreased below a threshold, $\dot{m}_{\rm crit}/\dot{m}_{\rm c} \sim 4\Delta r/r_{\rm in}$ (sec. 3.1).

On the other hand, if radiation feedback from accretion onto the star plays an important role in regulating the viscosity (and so accretion rate) in the disc, then temporarily suppressing accretion onto the star might cause the level of ionization to drop and drive the source back into quiescence.

A final question remains: why do some sources show the accretion instability and trapped disc behaviour and not others? The vast majority of outbursting neutron stars show long periods of quiescence, consistent with being driven by the ionization instability with $r_{\rm in}$ far from $r_{\rm c}$, rather than remaining trapped near $r_{\rm c}$. Of the two sources we have considered, IGR J00291+5934 has previously shown a normal outburst pattern (a much stronger outburst followed by a long quiescence; Hartman, Galloway & Chakrabarty 2010.

In their discovery paper for NGC 6440 X-2, Altamirano et al. (2010) remark that the short recurrence time and weak outburst likely cause similar NS sources to be missed by current surveys, so it is possible that such sources are common but remain undiscovered. As well, in DS11 we showed that the very small ratio $T_{\rm visc}/T_{\rm SD} \sim 10^{-17}$ for rapidly spinning pulsars made it more likely that the disc would become untrapped (with $r_{\rm in}$ moving rapidly away from $r_{\rm c}$) as $\dot{m} \rightarrow 0$. Hartman, Galloway & Chakrabarty (2010) suggested that the disc might remain weakly ionized during the entire outburst, which would then decrease the viscosity and increase $T_{\rm visc}$, perhaps enough to prevent the disc from becoming untrapped. If the RI instability is responsible for the 1Hz QPO seen in NGC 6440 X-2 and SAX J1808.4-3658, then the fact that only sometimes manifests is consistent with the idea that $\Delta r/r_{\rm in}$ is variable (since the instability only occurs over a small range in $\Delta r/r_{\rm in}$).

For T Tauri stars, the main constraint on the instability is the presence of a strong ($\sim$ 1 kG) dipolar magnetic field. Although most T Tauri stars show a strong surface field component, the dipo-

lar component can vary considerably, to the point that it is not clear whether the disc-field interaction considered here is primarily responsible for the low spin-rate of the star. The inclination between the rotation axis of the star and the magnetic field could also affect the instability by changing $\Delta r_2/r_{\rm in}$ (as above). This would suggest that, as a class, EXors are T Tauri stars with moderate accretion rates and strong, aligned dipolar magnetic fields compared with normal T Tauri stars.

7 CONCLUSIONS

As found in DS10, accretion from a disc onto a magnetosphere tends to take place in what we have called 'trapped' states. The inner edge of the disc hovers around the corotation radius in this state, even at very low accretion rates. The accretion in this state can be steady or cyclic. We have investigated here the conditions under which the cyclic form takes place, the kinds of cycles, their amplitudes, cycle periods and their effect on the average torque on the accreting star.

Two forms of cycle are found; the first form (labeled RI here) is the accretion/dead disc cycle already suggested by Sunyaev & Shakura (1977). A pile-up of mass at the 'centrifugal barrier' outside corotation is followed by an episode of accretion emptying the pile and the beginning of a new cycle. Mass loss or 'propellering', whether it takes place or not, is a separate piece of physics not needed for understanding the effect of a centrifugal barrier on a viscous disc accreting on a magnetosphere.

Whether accretion is cyclic or continuous is found to depend on the width of the transition from an accreting state (inner edge inside corotation) to a suspended accretion state (edge outside corotation). A narrow width leads to RI cycles, a broader transition to continuous accretion. The effect of these cycles is to increase the average spindown torque on the star. A second form of cycle takes places when the average accretion rate is close to the standard accreting case (edge inside corotation). It decreases the average torque on the star.

A review of the available literature shows forms of variability that may be related the the cyclic forms of accretion found here, the most promising ones may be the 'EX Lup' outbursts, and a new form of cyclic accretion found in X-ray binaries NGC 6440 X-2 and SAX J1808.4-3658.

8 ACKNOWLEDGMENTS

CD'A acknowledges financial support from the National Science and Engineering Research Council of Canada, and thanks Attila Juhasz for interesting dicussions and the use of figure 12.

REFERENCES

Agapitou V., Papaloizou J. C. B., 2000, MNRAS, 317, 273
Altamirano D. et al., 2010, ApJ, 712, L58
Aly J. J., 1985, A&A, 143, 19
Aspin C., Reipurth B., Herczeg G. J., Capak P., 2010, ApJ, 719, L50
Bildsten L. et al., 1997, ApJS, 113, 367
Camero-Arranz A., Finger M. H., Ikhsanov N. R., Wilson-Hodge C. A., Beklen E., 2010, ApJ, 708, 1500
Chakrabarty D. et al., 1997, ApJ, 481, L101+
D'Angelo C. R., Spruit H. C., 2010, MNRAS, 406, 1208
—, 2011, MNRAS, 416, 893
Davidson K., Ostriker J. P., 1973, ApJ, 179, 585
Donati J. et al., 2008, MNRAS, 386, 1234
Dullemond C. P., Monnier J. D., 2010, ARA&A, 48, 205
Fromang S., Stone J. M., 2009, A&A, 507, 19
Getman K. V., Feigelson E. D., Micela G., Jardine M. M., Gregory S. G., Garmire G. P., 2008, ApJ, 688, 437
Goodson A. P., Winglee R. M., Boehm K., 1997, ApJ, 489, 199
Hartman J. M., Galloway D. K., Chakrabarty D., 2010, ArXiv e-prints
Hayashi M. R., Shibata K., Matsumoto R., 1996, ApJ, 468, L37+
Heinke C. O. et al., 2010, ApJ, 714, 894
Herbig G. H., 2007, AJ, 133, 2679
—, 2008, AJ, 135, 637
Illarionov A. F., Sunyaev R. A., 1975, A&A, 39, 185
Lasota J., 2001, New Astron. Rev., 45, 449
Miller K. A., Stone J. M., 1997, ApJ, 489, 890
Muzerolle J., D'Alessio P., Calvet N., Hartmann L., 2004, ApJ, 617, 406
Patruno A., Watts A., Klein Wolt M., Wijnands R., van der Klis M., 2009, ApJ, 707, 1296
Patruno A. et al., 2010, The Astronomer's Telegram, 2672, 1
Perna R., Bozzo E., Stella L., 2006, ApJ, 639, 363
Pringle J. E., Rees M. J., 1972, A&A, 21, 1
Romanova M. M., Kulkarni A. K., Lovelace R. V. E., 2008, ApJ, 673, L171
Romanova M. M., Ustyugova G. V., Koldoba A. V., Lovelace R. V. E., 2004, ApJ, 616, L151
—, 2009, ArXiv e-prints
Sipos N., Ábrahám P., Acosta-Pulido J., Juhász A., Kóspál Á., Kun M., Moór A., Setiawan J., 2009, A&A, 507, 881
Spruit H. C., Taam R. E., 1993, ApJ, 402, 593
Sunyaev R. A., Shakura N. I., 1977, Pis ma Astronomicheskii Zhurnal, 3, 262